Analyzing 23 years of warm-season derechos in France: a climatology and investigation of synoptic and environmental changes

Lucas Fery[1,2,*] and Davide Faranda[1,3,4,*]

[1]Laboratoire des Sciences du Climat et de l'Environnement, UMR 8212 CEA-CNRS-UVSQ, Université Paris-Saclay, IPSL, 91191 Gif-sur-Yvette, France
[2]SPEC, CEA, CNRS, Université Paris-Saclay, F-91191 CEA Saclay, Gif-sur-Yvette, France
[3]London Mathematical Laboratory, 8 Margravine Gardens London, W6 8RH, UK
[4]Laboratoire de Météorologie Dynamique/IPSL, École Normale Supérieure, PSL Research University, Sorbonne Université, École Polytechnique, IP Paris, CNRS, Paris, 75005, France
[*]These authors contributed equally to this work.

Correspondence: Lucas Fery (lucas.fery@lsce.ipsl.fr)

Abstract. A derecho is a type of severe convective windstorm characterized by a swath of severe wind gusts several hundred of kilometers long. Such storms are known for there potential to cause widespread damage and for there threat to infrastructures and people, particularly in the United States of America (USA). Although less frequent, derechos also occur in Europe. A recent example is the derecho of 18 August 2022 that produced damaging surface wind gusts (>200 km/h) and affected Corsica, Italy, Slovenia, Austria and Czech Republic within 12 hours. In this study we create a first climatology of recent warm-season derechos in France. We identified twenty-nine (29) events between 2000 and 2022 (23 years) using severe wind gust reports and satellite imagery. Derechos in France are much less frequent and intense than in the USA, but are more similar to those in Germany. Some differences exist with more frequent events in August and a larger proportion of short-lived low-end intensity events. In a second part, we analyse changes in synoptic conditions and environmental convective parameters associated with past warm-season derechos. To do so, we compare atmospheric circulations encoded in the 500 hPa geopotential height patterns associated with derechos in a relative distant past (1950-1980), when warming was still limited, and in a recent past (1992-2022). For the majority of the events, we find a significant signal of increased convective available potential energy (CAPE) consistent with overall trends in the Mediterranean basin while we find inconsistent changes in wind shear in the recent period. These changes are almost always correlated with higher near-surface temperatures and shifts in the mid-level atmospheric flow patterns and often associated with increased rainfall volume. It remains unclear to what extent those changes are attributable to anthropogenic climate change as we cannot rule out the influence of factors of natural variability such as the El-Nino Southern Oscillation (ENSO) or the Atlantic Multidecadal Oscillation (AMO).

1 Introduction

The term "derecho" (Hinrichs, 1888) is used to describe convective storm episodes that are characterized by a particularly long-lasting and widespread production of damaging downbursts. More specifically, a derecho is usually defined as "any family of downburst clusters produced by an extratropical mesoscale convective system (MCS)", following Johns and Hirt (1987).

The associated radar signatures generally have linear characteristics, with bow echoes (Fujita, 1978). Derechos are often subcategorized in "serial" or "progressive" type derechos (Johns and Hirt, 1987; Squitieri et al., 2023; Corfidi et al., 2016). A "progressive" derecho is characterized by a fast-moving MCS with a long-lived bow echo pattern on radar display, almost perpendicularly oriented with respect to the mean wind direction and usually occurs in the warm season (May-August). This type of derecho often move faster than the mean wind and is associated with high instability. Other common features include rear-inflow jet and mesoscale vortices. The other type of derecho, "serial" derecho, typically features an extensive squall line with a line echo wave pattern (LEWP) oriented embedded within a cold front. This type of derecho usually occur in the cold season (September - April) in an environment characterized by strong forcing and low instability. Those convective systems move typically more slowly than the "progressive" derechos.

Different criteria have been used to define a series of downburst clusters as a derecho from observational data such as wind gusts reports and weather radar. For instance, Johns and Hirt (1987) proposed the following criteria i) a concentrated area of convective wind-gusts nature with a speed greater than or equal to 26 m/s or – when wind-speed measurements are not available – the presence of damage following downbursts. The major axis length must be of at least 400 km; ii) the convective gusts must have an identifiable spatio-temporal progression, iii) at least 3 gusts greater than or equal to 33 m/s must be measured or assessed on the basis of damage within the area covered by the episode and these reports must be separated by at least 64 km from each other; iv) there must be no interruption of more than 3 hours between two successive severe wind gusts reports; v) the associated convective system must have temporal and spatial continuity in surface pressure or wind field; vi) all the wind gusts reports must emanates from the same MCS based on radar data.

However, later studies have often relaxed and/or modified some of these criteria and particularly the most restrictive one (iii) as it was argued there is no reference to wind threshold criteria in the common definition of derecho as a family of downbursts clusters Bentley and Mote (1998); Fujita and Wakimoto (1981). Coniglio and Stensrud (2004), Bentley and Mote (1998) and Gatzen et al. (2020) for instance, have not retained this criterion and instead assigned an intensity to the event depending on the number of reports of wind gusts at different thresholds (moderate intensity when there at least 3 reports of wind gusts greater than 33 m/s, high-end intensity when there at least 3 reports of wind gusts greater than 38 m/s, and low-end intensity otherwise). In 2016, Corfidi et al. (2016) proposed a more restrictive definition of derecho which includes only the most severe, long-lived "progressive" or warm-season derechos, as the dynamics and environments associated with "progressive" and "serial" derechos are very different. In particular, “The damage swath must be nearly continuous, at least 100 km wide along most of its extent, and 650 km long”. This definition also requires some clear evidence of radar features such as bow echoes, mesoscale vortices and rear-inflow jets. For a review of research on derechos including the different set of criteria used in the past studies, see e.g. Squitieri et al. (2023).

The derechos are phenomena that are mainly documented in the United States of America, and particularly in the Midwest and Southern Plains (Hinrichs, 1888; Johns and Hirt, 1985, 1987; Bentley and Mote, 1998; Evans and Doswell, 2001; Coniglio and Stensrud, 2004; Ashley and Mote, 2005; Guastini and Bosart, 2016). In comparison, the science of derechos is more recent in Europe, as events have only started to be reported as such since the 2000s (López, 2007; Gatzen, 2004; Punkka et al., 2006; Púčik et al., 2011; Hamid, 2012; Celiński-Mysław and Matuszko, 2014; Mathias et al., 2019) and few national climatologies have been established (Gatzen et al., 2020; Celiński-Mysław et al., 2020). In particular, there is not to our knowledge any previous work studying the climatology of derechos in France although several cases have been reported in scientific articles (López, 2007; Gatzen et al., 2020; Hamid, 2012), or weather reports such as those from Keraunos, the French observatory of severe convective storms (website: https://www.keraunos.org/). For these reasons, the public opinion was astonished at the violence and the widespread destruction of the derecho that affected Corsica in summer 2022. This MCS formed during the night of August 17 to 18 over the northern Balearic Islands as an initial line of thunderstorms gradually curved to become a bow echo and moved rapidly to the northeast, affecting Corsica in the early morning. The system then affected central and northern Italy, Slovenia, Austria and Czech Republic, within 12 hours. The storm occurred in synoptic conditions featuring a meridional circulation with the presence of a cut-off low located between Portugal and France, a pattern associated with the so-called Spanish plume (Morris, 1986; Holley et al., 2014) and an anticyclone over the Mediterranean basin. Such a cut-off low typically produces heatwave or stormy conditions over France when positioned respectively over the Eastern Atlantic or Portugal or over Spain. In particular, the convective system was maintained by the particularly warm sea-surface temperatures (SST) of the Mediterranean sea and convection produced intense downbursts with up to 225 km/h surface wind gusts recorded over Corsica. With 12 casualties, over 100 people injured and disruption of electric power lines (Wikipedia, 2022), there was immediate questioning about whether this exceptional storm was unique or other similar events have occurred in the past, and whether climate change had played a role in favoring this event. While the warming of the Mediterranean Sea (with anomalies up to +6°C recorded during the summer with respect to the seasonal values for the period 1990-2020) has very likely promoted the development of 2022 European derecho, an assessment of the role of human-induced climate-change on the occurrence of the severe convective events is a difficult task, particularly when interested in convective winds (Kunkel et al., 2013). Because of their scarcity and the computational cost of simulating mesoscale convective events in global and regional climate models, it is difficult to find clear climate change statements about severe convective storms, including derechos. Due to these modelling difficulties, even the IPCC reports do not contain much strong statements about the influence of anthropogenic climate change on severe convective events. Indeed, in the AR6 report (IPCC, 2021), we find that there is high confidence that "a warmer climate intensifies very wet and very dry weather events and seasons, but the location and frequency of these events depend on projected changes in regional atmospheric circulation". Particularly for Europe, there is moderate confidence that at 1.5°C of warming, "heavy precipitation and associated flooding are projected to intensify and be more frequent", and low confidence that "large-scale conditions conducive to severe convection will tend to increase in the future climate".

Some studies have investigated the existence of changes in MCS frequency and intensity (Schumacher and Rasmussen, 2020), environmental predictors for convection such as CAPE and wind shear (Taszarek et al., 2021b, a; Púčik et al., 2017) or convective hazards (Battaglioli et al., 2023) with global warming. Generally, the results show important regional discrepancies. There is however general agreement that rainfall rate and volume associated with MCS tends to increase with global warming. For midlatitudes and Europe, CAPE has been shown to increase and 0-6 km wind shear has been shown to slightly decrease (Taszarek et al., 2021b). However, convective inhibition (CIN) also tends to increase, and relative humidity tends to decrease which makes difficult any statement about the frequency of severe thunderstorms as pointed out by Taszarek et al. (2021a);

Natalia Pilguj et al. (2022). The lack of clear results about the frequency of severe convective storms under anthropogenic climate change, including derechos, also motivates the analysis presented in this study.

The first purpose of this paper is to establish a first climatology of recent warm-season derechos in France and analyse their features in comparison with other countries. The second goal is to identify potential changes in synoptic conditions and environmental convective parameters such as convective available potential energy (CAPE) and bulk wind shear associated with past derecho-producing MCS in the warm-season in France and assess the role of climate change and natural variability in accounting for these changes.

We present in Section 2 the methodological aspects of this work and introduce the datasets we use: in 2.1, we present the methodology and observational datasets used to detect past derechos events over France and its limitations; in 2.2, we introduce the attribution methodology based on analogues of synoptic patterns, the reanalysis or observational datasets used and we introduce the relevant assessment metrics. The results are presented in Section 3 for: the detected derechos and the analysis of their frequency, intensity and geographical distribution in comparison with established climatologies in Germany or the Unites States of America (USA) (3.1); the attribution for the case of 2022 derecho in detail (3.2); the overall attribution for all events, with their interpretation (3.3). Finally, we conclude on the results and limitations of this study and we discuss the perspectives for future work in Section 4.

2 Data and Methods

2.1 Derechos detection

Similarly to Gatzen et al. (2020) who established a climatology of derechos over Germany between 1997 and 2014, we use daily weather station data from Météo-France (automatic stations of type 0 and 1) to do a first selection of the warm-season days (May, June, July, August) with at least 5 stations reporting a severe daily wind gusts (measured wind speed greater than 25 m/s). We then filter out the days when no concentrated area of wind gusts reports is found i.e. when the reports are spread out across the map meaning there are likely not generated by a single MCS. In case they are missing because of an unsufficient number of reports, we also includes days for which a derecho has been reported over France by (Gatzen et al., 2020). Then we use the Python FLEXible object TRacKeR (PyFLEXTRKR) algorithm developed by Feng et al. (2023a) to systematically detect and track potential associated MCS for each previously selected day. This algorithm has notably been used to build a global MCS database Feng et al. (2021) using satellite imagery data, namely brightness temperature and precipitation. It has also been used to track MCS in convection-permitting simulations Feng et al. (2023b) or convective cells from radar data Feng et al. (2022). For the detection and tracking of MCS, the algorithm uses brightness temperature thresholds to identify cold cloud systems ($T_b < 241\,\mathrm{K}$) with an additional size constraint of an area $> 4 \times 10^4\,\mathrm{km}^2$. Precipitation data is used in addition to enable a more robust identification of MCS by requiring that an intense precipitation feature (criteria includes rain rate $> 3\,\mathrm{mm/h}$ and major axis length $> 100\,\mathrm{km}$) is embedded within the cold cloud system. These criteria must be met for at least 4 hours to define a cold cloud system as an MCS. We specifically use the Global Precipitation Measurement (GPM) Integrated Multi-satellitE Retrievals (IMERG) V06 precipitation database (Huffman et al., 2019) and the NOAA NCEP/CPC

Global Merged IR (MERGIR) brightness temperature (T_b) database (Janowiak et al., 2017), as in Feng et al. (2021). Both datasets are available from the year 2000 and cover the area between 60°S and 60°N at a time resolution of 30 minutes. The MERGIR database has a finer resolution (4km) than IMERG (10 km/0.1°), so we regridded T_b data to a resolution of 0.1° using xESMF python package (Zhuang et al., 2023) prior to applying the tracking algorithm.

Contrary to Coniglio and Stensrud (2004) and Gatzen et al. (2020) who used radar data to identify the convective system, we decided to use satellite data which are more easily accessible (from e.g. https://disc.gsfc.nasa.gov/) and have a global coverage. Indeed, radar data are often acquired, managed and hosted by national weather services and consequently cover only national geographical domains. Moreover, these data are often not easily and freely accessible. As we focus on warm-season derechos, the use of radar data is less critical than for cold-season derechos whose downbursts are difficult to disentangle from the associated synoptic-scale winds (Gatzen et al., 2020), and Coniglio and Stensrud (2004) found that the associated MCS were identified quite well without radar data. Nevertheless, radar data would be necessary to check the existence of a well-organized mesoscale convective system (e.g. with bow echoes), to make sure the wind gusts emanates from the same convective system and to match precisely the timestamps of wind gusts reports and the position of the convective system. Thus, our methodology have some limitations as we could define as a derecho a swath of wind gusts emanating from a disorganized convective cluster that doesn't feature a well organized structure on radar display or from one or several supercells, although there has been some debate about whether the specific structure of the convective system that produces the swath of severe wind gusts should or not be taken into account to define a derecho-producing MCS (Coniglio and Stensrud, 2004; Bentley et al., 2000).

The MCS detected using PyFLEXTRLR are then matched in time and space to the severe wind gusts reports from Météo-France weather stations and only the days when reports can be matched with an MCS along a distance of at least 400 km are retained. To circumvent the limited geographical coverage of wind reports to France, we use severe wind gusts reports from the European Severe Weather Database (ESWD) database (accessible at https://eswd.eu/) created by the European Severe Storm Laboratory (ESSL) (Dotzek et al., 2009) whenever the associated MCS track extends in other countries. This database provides detailed and quality-controlled reports from severe convective events in Europe including severe wind gusts, heavy rain, hail, tornadoes, and damaging lightnings from a variety of sources. For our study, we only retained reports at level quality QC1 ("report confirmed by reliable source"). The reports can come from weather stations, in which case the wind gust speed is given, or by reports from wind gust damage report such as fallen trees, which doesn't allow a precise estimation of the wind gust speed and this is also a limitation, notably for the estimation of the derecho intensity.

2.2 Detection of changes in synoptic patterns

To understand how anthropogenic climate change may have influenced the synoptic patterns related to severe convective events like derechos, we consider analogues of patterns of atmospheric circulation. Although there is no one-to-one correspondence between large scale synoptic patterns and the occurrence of derechos, the former are typical recurrent large scale conditions that are associated with favorable environment for the development of severe convective events (Bentley et al., 2000; van Delden, 2001; Coniglio et al., 2004; Lewis and Gray, 2010; Markowski and Richardson, 2010; Yang et al., 2017). To investigate this, we are examining changes in temperature, precipitation, wind speed, along with proxies or environmental parameters that are commonly used as predictors for convection, namely convective available potential energy (CAPE) and 0-6 km wind shear (named hereafter deep layer shear or DLS) (Taszarek et al., 2020, 2019) by identifying similarities between large-scale geopotential height fields at 500 hPa associated with historical derechos in the past (1950-1980) and the recent past (1992-2022). Our assumption is that the past serves as a hypothetical world where the Earth's climate was only marginally affected by human activity, and that 30 years is a sufficient period to account for natural variability in atmospheric motions. However, we must also consider long-term natural variability such as that caused by the Atlantic Multidecadal Oscillation (AMO) or El Niño-Southern Oscillation (ENSO). If a direct influence of such low-frequency variability is excluded, then changes in analogues between the two periods we consider can be attributed to the climate change signal. The method ensures that comparisons are relevant, unlike purely statistical modeling techniques, which aim to analyze meteorological variables without tracing them back to the phenomena that produce them - a thunderstorm or hurricane, for example. In addition, this method allows us to determine when a weather event is unprecedented because of an atmospheric circulation that has never been observed in the past making it statistically impossible to say whether climate change has made the event more likely.

We specifically compare the 1992-2022 geopotential height patterns at 500 hPa (Z500) fields to fields from 1950-1980, when warming was much more limited. To account only for the atmospheric circulation which is determined by Z500 gradients we remove the offset of geopotential height which has a trend linked with anthopogenic climate change Christidis and Stott (2015). To do so, we substract the mean value of each Z500 field to remove the mean thermodynamic contribution of global warming and focus on dynamical changes in the Z500 gradient which is directly linked to the quasi-geostrophic flow. These Z500 analogues reflect the mid-level large-scale dynamics that controls environmental conditions which can drive extreme events such as heat waves, cold waves, MCS outbreak, medicanes, tropical and extratropical cyclones and, in the present case, MCS associated with derechos. Nevertheless, one should keep in mind that sub-synoptic scale environments such as fronts also play a key role in the development of convective storms, particularly when it comes to convective initiation and the release of latent CAPE (Markowski and Richardson, 2010).

The attribution protocol described in Faranda et al. (2022) has already been applied and validated for pressure maps leading up to a series of extreme events in the year 2021, including winter storm Filomena, the French spring cold wave, the Westphalian floods, the Mediterranean summer heat wave, Hurricane Ida, the Po Valley tornado, medicane Apollo, and the Scandinavian late fall cold wave. Here we apply it for the first time to the synoptic patterns associated with historical derechos.

We use daily averaged Z500, wind speed, 2-meters temperature, and consider daily cumulative precipitation, daily maximum CAPE and DLS computed from ERA5 (Hersbach et al., 2018) hourly fields. ERA5 is the latest climate reanalysis produced by the European Centre for Medium-Range Weather Forecasts (ECMWF) as part of the implementation of the EU-funded Copernicus Climate Change Service (C3S). It provides hourly data on atmospheric, land surface and sea state parameters from 1950 to the present. The ERA5 data are available on the C3S Climate Data Store on regular latitude-longitude grids at a horizontal resolution of 0.25°×0.25°. Our choice of using ERA5 data for this study is firstly motivated by the consistency of the dataset through a long period of time (73 years) which enables the possibility of detecting changes in the large dynamics. Moreover, the global nature of this datasets allows to avoid the problems of mixing data-sets from different national weather services and ensures a uniform spatial and temporal coverage. However, there are some caveats due to the long-term improvement of observation instruments including satellites that can affect the uniformity of the quality of the dataset and potentially induce spurious trends.

We also consider 2-meters temperature and accumulated rainfall from the E-OBS observational dataset v27.0 (Cornes et al., 2018), available from https://www.ecad.eu/download/ensembles/download.php which interpolates measurements from land weather stations across Europe on a regular grid at 0.1° resolution.

We divide the datasets into two periods: 1950-1980 and 1992-2022 each consisting of 30 years of daily data. We consider the first period to represent the equivalent of a "counterfactual" world with a weaker anthropogenic influence on climate than the second period, which represents our "factual world" significantly affected by anthropogenic climate change. Here, we assume that 30 years is a long enough period to average out high-frequency interannual variability of the atmospheric motions. This time period is also recommended by the WMO for the computation of climate normals (Arguez and Vose, 2011). To account for the possible influence of low-frequency modes of natural variability in explaining the differences between the two periods, we also consider the possible roles of the El Niño-Southern Oscillation (ENSO), the Atlantic Multidecadal Oscillation (AMO), the Pacific Decadal Oscillation (PDO), the North Atlantic Oscillation (NAO), the East Atlantic (EA) and Scandinavian (SCAND) North Atlantic patterns. The NAO, the EA and to a lesser extent ENSO have been found to have a significant role in modulating extreme precipitation events in some regions of Europe (Nobre et al., 2017). The role of AMO has been discussed, e.g., in Zampieri et al. (2017) who found an influence on pressure, precipitation and temperature patterns. Wei et al. (2021) found an influence of PDO on northwestern Europe extreme rainfall. Similarly, Casanueva et al. (2014) found a significant role of SCAND in autumn and spring on extreme precipitation in Europe.

For each period, we examine all daily averaged Z500 maps and select the best 29 analogues, i.e. the maps minimizing the Euclidean distance to the event map itself. The number of 29 corresponds approximately to the smallest 3‰ Euclidean distances in each subset of our data. We tested the extraction of 25 to 50 analogous maps, without finding qualitatively important differences in our results. For the factual period, as is customary in attribution studies, the event itself is suppressed. In addition, we prohibit the search for analogues within a one-week window centered on the date of the event. We also restrict the search for analogues to the season in which each event occurs (in this case the warm season : May, June, July and August). This allows us to identify possible changes in seasonality — defined as the relative frequency of analogues occurrence per calendar month — between the counterfactual and factual periods, while avoiding confounding the different physical processes that may contribute to a given class of extreme events during warm and cold seasons.

Finally, we examine the seasonality of the analogues during the relevant season and their association with factors of natural variability (ENSO, AMO, PDO, NAO, EA, SCAND). We perform this last analysis using monthly indices from NOAA/ERSSTv5 data and retrieved from the Royal Netherlands Meteorological Institute (KNMI) Climate Explorer (accessible at https://climexp.knmi.nl/selectindex.cgi). In particular, the ENSO index is version 3.4 as defined by Huang et al. (2017), and the AMO index is calculated as described in Trenberth and Shea (2006). To assess the possible association of these different indices on circulation changes between factual and counterfactual periods, we compare the distributions of each index for the analogues of the two periods and we evaluate any significance changes between factual and counterfactual distributions by performing a two-tailed Cramér-von Mises test (Anderson, 1962) at the 0.05 significance level. If the p-value is smaller than 0.05, the null hypothesis (H = 0) that both samples are from the same distribution is rejected, and the influence of internal variability cannot be excluded. All relevant figure panels display the p-value (pval) and the H-test result in the title. Finally, we also compute the best 3‰ analogues for all the 1950-2022 Z500 dataset, without dividing it into factual and counterfactual periods and estimate a linear trend. Note that for this global quantile the total number of analogues in all decades amounts to 71. We compute the confidence interval of such a trend using the Wald method (Stein and Wald, 1947) in order to assess significance of the trends.

Following Faranda et al. (2022), we define certain quantities that support our interpretation of analogue-based assignment. All these quantities can then be compared between the counterfactual and factual periods.

- **analogue quality Q**: Q is the average Euclidean distance of a given day from its 29 closest analogues. If the value of Q for the extreme event belongs to the same distribution of its analogues then the event is not unprecedented and the attribution can be performed, if the value of Q is greater than those of its analogues the event is unprecedented and therefore not attributable.

- **Predictability Index D.** Using dynamical systems theory (Freitas et al., 2011, 2016; Lucarini et al., 2016), we can compute the local dimension D of each Z500 map (Faranda et al., 2017a, 2019). The local dimension is a proxy for the number of degrees of freedom of the field, meaning that the higher D, the more unpredictable the temporal evolution of the Z500 maps will be (Faranda et al., 2017b; Messori et al., 2017; Hochman et al., 2019). If the dimension D of the derecho event analyzed is higher or lower than that of its analogues, then the extreme will be respectively less or more predictable than the closest dynamical situations identified in the data.

- **Persistence index** Θ: Another quantity derived from dynamical systems theory is the persistence Θ of a given configuration (Faranda et al., 2017a). Persistence estimates the number of days we are likely to observe a map that is an analogue of the one under consideration (Moloney et al., 2019). As with Q and D, we compute the two values of persistence for the extreme event in the factual and counterfactual world and the corresponding distributions of the of persistence for the analogues.

- **Seasonality of analogues**: We can count the number of analogues in each month to detect whether there has been a shift in circulation to months earlier or later in the season. This can have strong thermodynamic implications, for example if a circulation leading to large positive temperature anomalies in early spring becomes more frequent later in the season, when average temperatures are much higher.

- **Association with factors of natural variability**: To account for the effect of natural inter-decadal variability, we analyze the distributions of ENSO, AMO, PDO, NAO, EA and SCAND indices corresponding to the analogues of each event in the factual and counterfactual periods. If the null hypothesis that the two distributions do not differ between the two periods is rejected, we cannot rule out that the thermodynamic or dynamical differences in the analogues are partly due to these modes of natural variability, rather than anthropogenic forcing. On the other hand, if the null hypothesis of equal distributions cannot be rejected, the observed changes in the analogues are attributed to human activity.

3 Results

3.1 Detected derechos over France between 2000 and 2022

In total, we found twenty-nine (29) warm-season derechos that occurred over France between 2000 and 2022. A summary of the identified derechos with their start date and time, their path length, duration, intensity and affected countries is presented in Table 1. Additionally, we provide a figure with wind gusts reports in France and the path determined from the first and last reports of each derecho in supplementary material. Just like Gatzen et al. (2020), we compute for each derecho its path length as the distance between the first and last severe wind gust reports, and the duration as the time elapsed between these two reports. We also define the intensity as in Gatzen et al. (2020); Coniglio and Stensrud (2004) from the observed number of wind gusts reports above thresolds : if there at least 3 reports $\geq 38\,\mathrm{m\,s^{-1}}$, the event is classified as high-end, if there are at least 3 reports $\geq 33\,\mathrm{m\,s^{-1}}$, the event is classified as moderate and the others that do not satisfy these criteria are classified as low-end.

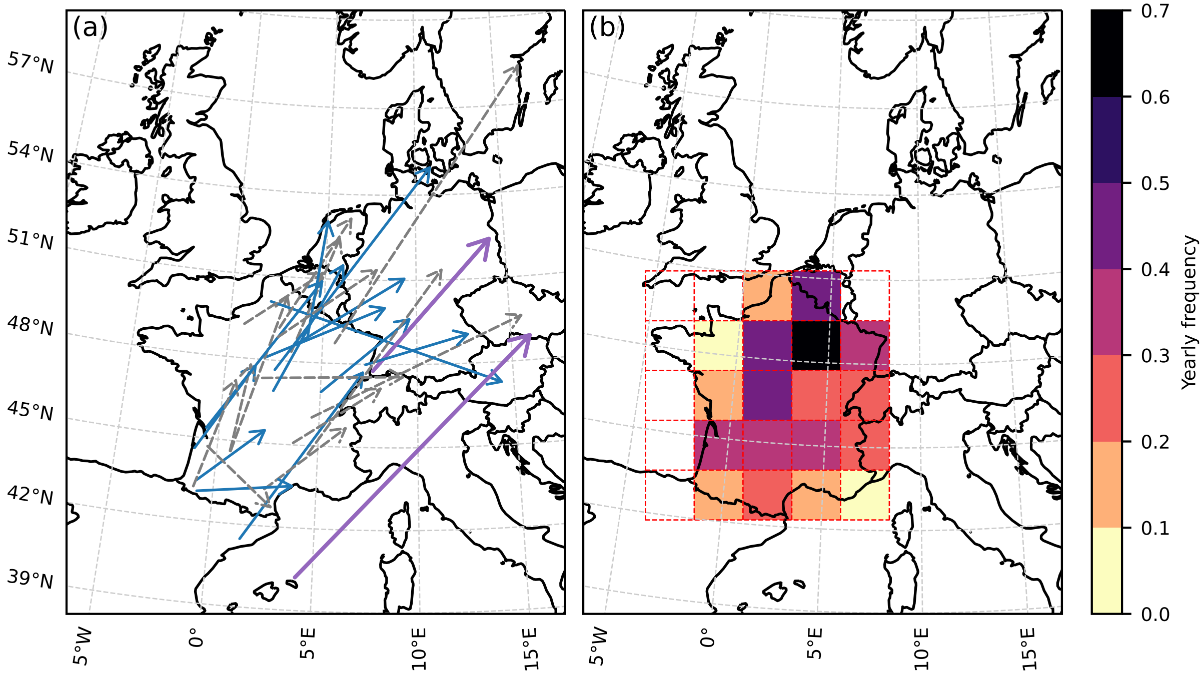

Figure 1. (a) Tracks of warm-season derechos that affected France between 2000 and 2022 depicted by arrows. The thin broken grey lines, thin blue lines, thick purple lines respectively represent low-end, moderate and high-end intensity derechos. (b) Heatmap of the yearly frequency of warm-season derecho computed for geographical squares of dimensions 200 km $\times$ 200 km.

Compared to Germany, we observe a slightly more frequent occurrence of warm-season derechos in France (1.26 event per year vs 1.22 per year) overall but France is about 50 % larger than Germany. Relative to the size of Germany, the observed frequency of warm-season derechos is lower in France (0.82 event per year). However there are important regional discrepan-

Number	Start date and time (UTC)	Path length (km)	Duration (h)	Intensity	Affected countries
1	2000-07-02 13:55	560	7	moderate*	FR, DE
2	2001-07-06 16:45	500	6	moderate*	FR, DE
3	2001-08-15 13:15	700	10	low	FR, BE
4	2003-05-19 12:45	960	8	low	FR, CH, DE, CZ
5	2003-06-14 05:17	1000	15	moderate*	FR, DE, AT
6	2003-07-15 17:27	460	7	moderate	FR
7	2003-08-17 07:30	900	12	moderate	FR, CH, ES
8	2003-08-28 18:45	460	5	low	FR, CH
9	2004-08-17 14:42	450	6	low	FR
10	2005-07-29 14:27	690	10	high*	FR, CH, DE
11	2006-07-04 19:33	410	4	low	FR
12	2009-05-25 21:42	540	5	low	FR, BE, NL
13	2010-07-12 04:30	1050	13	moderate*	FR, BE, LU, NL, DE, DK
14	2010-07-14 12:11	580	8	moderate*	FR, BE, NL, DE
15	2011-06-22 13:08	470	5	moderate*	FR, CH, DE
16	2012-06-07 11:24	600	7	low	FR, CH
17	2013-07-26 21:42	790	10	moderate	FR, BE
18	2013-07-27 16:23	620	7	moderate	FR, BE, NL, DE
19	2014-08-08 15:53	430	6	moderate	FR
20	2015-08-31 15:15	390	6	moderate	FR
21	2018-07-04 13:49	400	6	low	FR
22	2018-08-07 16:50	420	6	low	FR, BE, NL
23	2018-08-09 09:46	1350	18	low	FR, DE, DK, SE
24	2018-08-28 17:21	510	5	low	FR
25	2019-06-04 16:04	560	6	low	FR, BE, NL
26	2019-06-05 18:06	510	5	moderate*	FR, BE, NL
27	2021-06-19 16:18	520	8	low	FR, BE, LU, DE
28	2021-06-20 12:27	950	12	low	FR, CH, DE
29	2022-08-18 01:35	1400	16	high	FR, IT, SI, AU, CZ

Table 1. List of warm-season derechos that affected France between 2000 and 2022. Unless stated otherwise, intensity is assessed from reports in France only. * intensity assessed using not only weather reports from Météo-France but also reports outside of France (from ESWD or German Weather Service DWD (data accessible at https://cdc.dwd.de/portal)) or intensity assessment by Gatzen et al. (2020)

cies as can be seen on Figure 1(a) where we plot the trajectories of all derechos as the straight arrow linking the geographical locations of the first and last reports and 1(b) where we show the average number of warm-season derechos per year per 200 km $\times$ 200 km grid cells like in Gatzen et al. (2020) and Coniglio and Stensrud (2004), counting the number of events for which associated severe wind gusts are found in each cells. Indeed northeast of France have the highest frequency of events (culminating at 0.61 derechos per year) while Brittany (western part) has no event. This highest frequency is lower than the maximum frequency observed in Germany for the entire year and for moderate and high end events only (0.72 per year) so the frequency might be comparable for the warm season and all events. However, warm-season derechos are much more frequent in the USA with up to 1.9 event per year for equal size grid cell (Coniglio and Stensrud, 2004) in the Southern Plains or the Midwest (Guastini and Bosart, 2016). Most of the trajectories have a northeastern direction, in agreement with German warm-season derechos. Furthermore, looking at the daily averaged 500 hPa geopotential height pattern (shown for each event in supplementary figures), we mainly observe southwesterly flow associated with the events consistent with the preferred development of extratropical MCS ahead of a trough or a cut-off low Coniglio et al. (2004); Yang et al. (2017); Houze (2018); Gatzen (2004, 2013); Gatzen et al. (2020); van Delden (2001). From the map of trajectories, there seems to be 3 main typical paths for derechos in France: i) one type of path originates in the southwest in Nouvelle Aquitaine region and move in a north-northeast direction; ii) another type of path starts in the east or south and moves to the east-northeast to Switzerland and/or southern Germany stopping at the foot of the Alps, or passing north of the Alps, matching most of the warm-season events identified by Gatzen et al. (2020); iii) a last type begins in the center or northeast of France and moves through the northern plains to the north-northeast towards the Benelux and/or Germany. The 2022 derecho that affected Corsica stands apart as it originated near the Balearic islands in the Mediterranean sea and no similar event is found, but there could have been similar events that we didn't detect as Corsica is a rather small isolated region and there is no or few weather stations at sea it is difficult to detect such an event using our methodology. This derecho also affected many other countries including Italy and Austria so one should probably use station data from several Mediterranean countries, and/or include overwater stations like Gatzen et al. (2020) to study these derechos.

We present histograms of path length, duration, intensity, and month of occurrence of observed derechos on Figure 2. Most of the identified events are of low-end (48 %) or moderate (45 %) intensity with only 2 high-end intensity events (7 %) (Figure 2 (a)). In comparison with derechos identified by Gatzen, we found smaller fractions of moderate (54 %) and high-end (14 %) intensity events and larger fraction of low-end events (32 %). However, as previously noted, we assess the intensity using only weather stations reports in France in most of the cases, so by obtaining station data from other countries, one might obtain upgraded intensities. The average path length is 660 km, similar to the 620 km found for Germany cases, and we observe a large fraction of events having a rather short path length (66 %) i.e. shorter than the 650 km threshold suggested by Corfidi et al. (2016) to revise the definition of derechos, while medium ($650 \leq$ length ≤ 950 km) and long path length (> 950 km) have about the same fraction (17 % or 5 events each). We observe consistent results for the duration of the events with a majority of duration lower than 7 hours. From these results, that derechos in France are less frequent and intense than derechos in the USA (about 10 per year) as was also noticed in Germany (Gatzen et al., 2020). Regarding the start time of derechos (histogram not shown), we observe similar results as Gatzen et al. (2020) with a peak at near noon and a second one in the end in the afternoon with however a shift of the late afternoon peak later in the day (between 16:00 and 17:00 compared to between 15:00 and 16:00 in Germany) and more events starting in the night or the late evening. The derecho frequency is very dependent on the particular year as we observe up to 5 events in a single year in 2003, or 4 events in 2018 while we observe no events for some years (2002, 2007, 2008, 2016, 2017). Some events also happen successively as observed in Germany by Gatzen et al. (2020) with two successive events on 26 and 27 July 2013, on 4 and 5 June 2019 or on 19 and 20 June 2021 for instance. Interestingly, we do not observe a peak of occurrence in July as for derechos in Germany or USA Coniglio and Stensrud (2004), but similar occurrence frequency between July and August (34 % in each month). This is probably linked to the near presence of Mediterranean sea and Atlantic Ocean that are still a sufficient source of moisture and heat late in the season to enable significant instability and the development of severe convective storms while this is not the case far inland like in Germany of the Great Plains in the US. We indeed observe that 8 out of 10 events occurring in August, have initiated in the south, either close to the Bay of Biscay or the Mediterranean sea. It is indeed well known that southern France is prone to extreme convective rainfall episodes in the fall season Fumière et al. (2020); Ribes et al. (2019); Taszarek et al. (2019). This suggests we should perhaps include the month of September, and possibly October in the warm-season for studying derechos in southern Europe in future studies.

3.2 Results of attribution for the 18 August 2022 derecho

We begin by analyzing in detail the result of the attribution analysis using the analogues methodology for the 2022 Corsica derecho to show how the results in the different variables and metrics are interpreted. As described in Section 1, a MCS developed and moved to the northeast, affecting Corsica, Northern Italy, Slovenia, Austria and Czechia within 12 hours, with the production of strong wind gusts along a 1000 km axis along with severe hail and heavy rainfall in some locations. For a detailed meteorological report, see for example ESSL (2022). Figure 3 shows the wind reports from Météo-France in Corsica and the trajectory of the storm.

Figure 4 shows the results of the attribution study of the synoptic configuration associated with the episode. The Z500 field of the event (Figure 4a) has been used for the search of 29 analogues for the counterfactual and factual periods. Their average is displayed respectively in 4b,c). We observed some significant changes in the circulation pattern, namely a relative deepening of the low pressure system on the North Sea and a strengthening of the Eastern European high pressure system which reinforces the gradient and thus the mid-level wind downstream of the cut-off low. This change is consistent with higher temperatures over Eastern Europe while it is difficult to make any statement about which is one is the cause or the consequence. We also observe significant increase of temperature around the Mediterranean sea with no significant change over the sea itself for which one should probably look preferably at sea surface temperatures to see a signal. We observe a significant decrease of precipitation over Northern Italy and a significant increase in northeastern Europe which could be partly explained by the shift in the atmospheric flow. The same results are found for EOBS dataset (figures provided in supplementary material). When examining daily maximum CAPE (Figure 5), we observe a significant increase over the Mediterranean, matching well with the very large values observed in 18 August 2022. We note that ERA5 values for CAPE are unrealistically large for the 2022

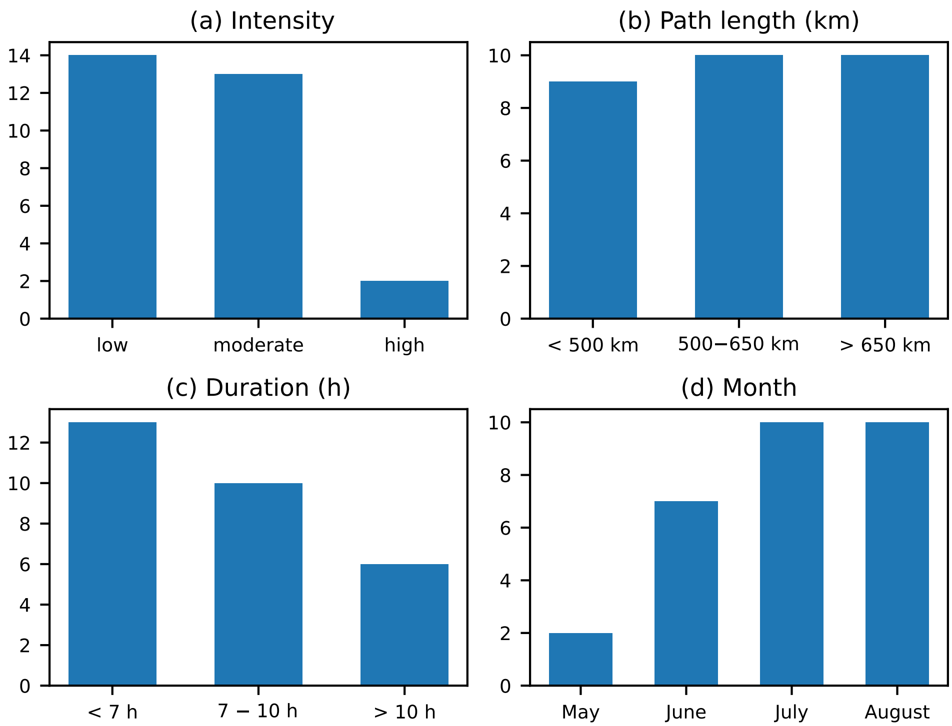

Figure 2. Statistics of observed warm-season derechos over France between 2000 and 2022. (a) Intensity defined from the number of reports exceeding given wind gusts speed thresholds (high : at least 3 reports $> 38\,\mathrm{m\,s^{-1}}$, moderate : at least 3 reports $> 33\,\mathrm{m\,s^{-1}}$, low : all remaining events). (b) Path length of derechos computed from the distance between first and last severe wind gusts reports. (c) Duration defined as the elapsed time between the first and last reports. (d) Month of occurence.

derecho (locally > 5000 J/kg), which is a known issue, highlighted in ERA5 documentation. As for deep layer shear 6, we find no significant signal along the path of the MCS.

The quality of the analogues (Figure 4q) shows that this circulation is relatively common compared to the rest of the analogues with no changes in the two periods. We do not detect visible changes in predictability D (Figure 4r) nor persistence Θ (Figure 4s) relative to the counterfactual world.

The seasonal occurrence of analogues (Figure 4t) is quite consistent with the months of thunderstorm occurrence in this area, with a maximum during August; however, we observe a small shift from June towards July.

The changes in ENSO (Figure 4u) are not statistically significant while AMO distributions have a significant shift between the two periods (Figure 4v) and so do the Scandinavian pattern (SCAND) (no shown here) suggesting a possible role of the natural variability in accounting for the observed changes. When comparing the patterns of sea-level pressure, surface temperature and precipitation characteristic of AMO in Europe (Zampieri et al., 2017) with the patterns of changes found here, we find a very good agreement suggesting that AMO might be the major factor explaining the observed changes. Finally, when

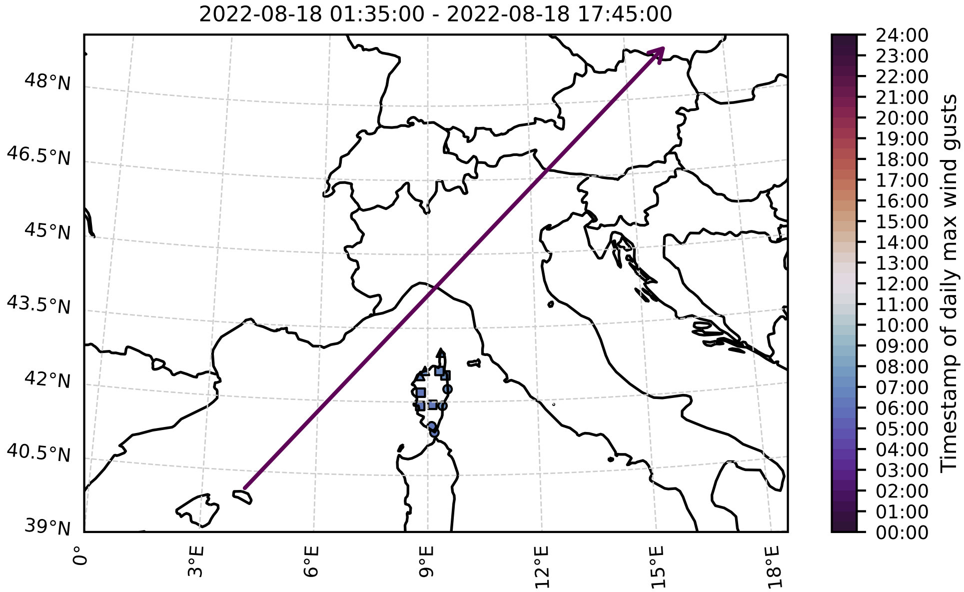

Figure 3. Trajectory of 18 August 2022 derecho and position of severe wind gusts reports from Météo-France in Corsica colored by their timestamp. The triangles represent extremely severe wind gusts ($> 38\,\mathrm{m\,s^{-1}}$), the rectangle represent medium severe wind gusts ($> 33\,\mathrm{m\,s^{-1}}$) and the circles represent other severe wind gusts ($> 25\,\mathrm{m\,s^{-1}}$). The time stamp of the first and last reports idenfied from ESWD are shown in the title.

computing analogues for the whole period and counting their frequency per decade, we observe no significant trend (Figure 4w).

3.3 Overall changes in synoptic patterns and environmental proxies

For each event, the same figures presenting the results of the attribution as for the 2022 event are provided in supplementary material. The overall results are summarized in Table 2. We show for each event whether there is a significant change or not in the distributions of analogues quality (average Euclidean distance to the best 29 analogues), dynamical indicators (local dimension D and persistence Θ) and indices of factor of natural variability (ENSO, NAO, AMO, PDO, EA, SCAND). For the dynamical indicators of analogues quality (Q), local dimension (D) and persistence (Θ) and for the frequency trend we specify the sign of the change in the mean value by "+" for an increase or "-" for a decrease, and we left the cell blank in case of no significant change. For atmospheric variables or parameters (t2m, tp for which we consider EOBS, and CAPE and DLS for which we use ERA5) we use the same notation. For natural variability indices, we put 1 when there is a significant change, and left the cell blank otherwise. We mark the same way significant changes in Z500 field which can feature complex changes in the synoptic configuration such as a dipolar or tripolar structure which translates into changes in the flow intensity and/or direction, including the jet stream.

Number	Q	D	Θ	Freq. trend	z500	t2m	tp	CAPE	DLS	ENSO	NAO	AMO	PDO	EA	SCAND
1		-			1	+	+		-		1	1	1		1
2					1	+	+	+						1	1
3				+	1	+	-	+		1			1		
4	-	-	-		1	+				1		1			1
5	-			+	1	+		+	+	1		1	1	1	
6			+		1		+	+		1			1	1	1
7	-				1	+	-	+		1		1	1		
8					1					1		1		1	1
9	-					+	+	+	+	1		1			1
10			-		1		+					1			
11		+	+		1	+	+	+		1	1	1	1		1
12	-				1	+	+	+		1		1			1
13	-				1	+	-	+	-		1	1			
14		+	-		1	+		+		1		1		1	1
15	-	-			1		+		+	1	1	1	1	1	1
16					1		+	+		1	1			1	
17	-		-		1	+			-			1			1
18			-		1	+			-	1		1	1		
19	-			+	1	+	+	+		1		1	1		
20					1				-						
21					1	+	-			1				1	1
22					1			+	+				1		
23	-		-	+	1	+		+		1	1		1		
24			-		1	+		+		1			1		
25	-			+	1	+	+	+		1	1	1			
26		+	-		1	+	+	+		1	1				
27			-		1	+	+	+		1	1	1		1	
28	+				1	+	+	+			1			1	
29					1	+	-	+				1			1

Table 2. Table showing the results of the attribution analysis with analogues. The columns are: Number: identification number for each derecho event; Q: analogue quality change: D: local dimension change; Θ: persistence change ; Frequency trend: trend in the number of analogues per decades (+ for increase, - for decrease, blank for no change); z500 (ERA5): changes in the Z500 pattern (1 if there are significant changes, blank otherwise); t2m (EOBS), tp (EOBS), CAPE (ERA5), DLS (ERA5): changes in those variables fields near the MCS path; ENSO, NAO, AMO, PDO, EA, SCAND: changes in the distribution of those natural variability indices between the two periods (1 if there is a significant difference, blank otherwise).

For 38 % of the events, we observe a significantly reduced average distance (Q) of each analogue compared to its own analogues, which might indicate that these patterns are more common in the recent period. However, this does not necessarily translates in a significant increasing trend frequency of the analogues. Indeed, there are only 5 events (17 %) for which we observe a significant increasing trend in the frequency of their Z500 analogues. The values are between 1.7 and 2.4 analogues per decade which is lower in average than the trends observed in average for the Z500 increasing patterns in the North Atlantic and Europe found in Faranda et al. (2023). Two (2) of the increasing patterns observed here (associated with the 2019-06-04 and 2001-08-15 events) match well with the composite of Z500 increasing patterns observed in this study. The pattern features a low-pressure anomaly in the Eastern Atlantic, off the coast of Britanny creating a southwesterly over the British Isles, which resembles the Spanish Plume, and a cut-off low over Greece. This suggests that this pattern known for its association with severe convective weather might become more common in the future.

We observe opposite results depending on the event for the local dimension (D), which is a proxy of predictability, with only three increasing and three decreasing cases. As for the persistence (Θ), we observe more often a significant decrease of persistence (30 %) of the patterns, while in (7 %) we observe an increase of persistence.

Apart one event for each no good analogue can be found (event n°12, 25 May 2009) – as the distance of the event to the best analogues is in the upper tail of the distribution – we find good quality analogues for all the events, which means the comparison between the analogues in the two periods is meaningful. However, we almost always notice significant changes in the Z500 field which implies we must be very careful in making attribution statements for the observed changes on the diagnostic variables (t2m, tp, CAPE and DLS).

For most of the events (76 %) we observe an significant increase of temperature, as expected with anthopogenic climate change an we observe no case with significant decrease, the remaining cases show no significant change. We also find in almost half cases (48 %) an increase of precipitation while small fraction (17 %) shows a decrease of precipitation. An increase of precipitation volume is in line with the projected increase of extreme precipitation in Europe IPCC (2021); Ribes et al. (2019), but one must keep in mind that here we are comparing average situations for a given circulation pattern, which do not necessarily each correspond to extreme precipitations events. In 69 % of the cases, we notice an increase in instability measured by CAPE and we don't find any decreasing case. This is in agreement with past findings about the increase of convective instability with global warming in the Mediterranean region Taszarek et al. (2021b). There are less significant results for DLS, with 14 % of decreasing cases and 17 % of increasing cases.

As for the influence of natural variability in accounting for these changes, we cannot rule out its influence on the observed changes. The most frequent factors involved are in the decreasing order ENSO (69 %), AMO (62 %), SCAND (45 %), PDO (41 %), EA and NAO (both 34 %).

When looking at relative frequency of occurrence in the months of the warm season (see supplementary figures, not shown in the table), the results are really case-dependant and it is thus difficult to make any general statement. More some patterns, we observe a relative increase of frequency in the late season with a decrease in earlier season and for some other patterns we observe an inverse tendency. More investigation would be needed to clarify those results, by e.g. making composites or clustering of the patterns with similar tendencies.

4 Conclusions

In conclusion, the study provides a 23-year climatology of warm-season derechos in France between 2000 and 2022. The events have been detected using wind gusts reports from weather station data (primarily from Météo-France and ESWD) and mapped with MCS detected using satellite imagery. We identified twenty-nine (29) events and analyzed their features in comparison with climatologies in the USA and Germany. Similarly to the observed derechos in Germany, warm-season derechos in France are much less frequent and intense than in the USA. Countrywide, we observe on average 1.26 derecho per year, while the highest local frequency is observed in northeastern France with about 0.6 derecho per year in a 200 km $\times$ 200 km grid cell. The frequency per standardized grid cell is similar but slightly lower than in Germany. Another difference is that events are more frequent in August in France the proportion of short-lived low-end intensity events is larger. As in Germany, warm-season derechos are associated with southwesterly flow and most of the storms move in a northeastern direction. Derecho-producing MCS in the warm-season tends to develop primarily in the center north, the southwest and the east but not much in the west.

We also investigated the potential role of climate change in modifying the characteristics of the atmospheric circulation and environmental conditions associated with historical derechos through the analogues of circulation patterns defined by 500 hPa geopotential height. We compared the weather patterns in a relative distant past (1950-1980) and in a more recent past (1992-2022). We observed significant increase of maximum daily CAPE, notably around the Mediterranean basin, and 2 m-temperature along with changes in the Z500 patterns for most events. Natural variability cannot be excluded in accounting for the observed changes, particularly the ENSO and AMO, for most events and further investigation is necessary to understand better the role of each of these factors and anthropogenic climate change.

It is important to note that this study has some limitations. Indeed, the methodology we used for the detection of derechos rely on semi-objective analysis, with a significant part of manual subjective decisions notably for the selection of days prior checking the existence of associated MCS and mapping the wind gusts reports with the MCS. The use of radar data would be useful to better assess the characteristics of the detected MCS which is diffult to do with satellite imagery because of the limited temporal and spatial resolution. Alternatively, or in complement, one could use lightning datasets such as EUCLID Schulz et al. (2016) to check the existence and track convective systems. Moreover, we mainly used weather stations data from Météo-France, which limits the accuracy of the detection near the national borders and while ESWD has proved very useful to provide severe wind gusts records and damage reports, it would be better to use other national station data or international SYNOP stations to precisely assess the intensity of each event and to improve the detection procedure. It would also be desirable to have an automated detection algorithm for detecting derechos as a manual identification is laborious and implies many flaws. Finally, a full-year climatology of derechos in France is still missing, and we could probably include the month of September in the warm-season for future studies. Based on the results and the limitations of this study, it is clear that further research is needed to better understand the statistics and dynamics of derechos and their potential link to climate change in France and Europe. Another area of focus could be gathering more detailed observations and data on the environmental conditions and dynamics associated with derechos using e.g. proximity soundings Evans and Doswell (2001); Gatzen et al. (2020), or model output from high-resolution reanalyses such as the forthcoming ERA6 or the analyses provided by nonhydrostatic convection permitting (Coppola et al., 2021) weather models such as WRF, ICON or AROME. Unfortunately we do not dispose of sufficiently long time series to use the existing data for the purpose of attribution.

Our attempt to analyse changes in synoptic conditions and convective environmental parameters characterizing instability (daily maximum CAPE) and wind shear (daily maximum 0-6 km wind shear or deep layer shear) and their potential links to natural variability and anthropogenic climate change has also some limitations and a more detailed analysis of the observed patterns associated with derechos is necessary to be able to make more convincing statements. This includes the clustering of the Z500 patterns to study similar patterns together and check if their trends are robusts. The study also does not take into account the potential impact of land use and land cover changes, as well as other surface variables including sea surface temperature (SST). The role of internal variability could be better assessed and quantified in linking derecho occurrence and the indices of those factors. These factors likely play a role not only in creating more or less favorable environments as we have seen for the role of AMO in the 2022 derecho case, but also in modulating the frequency of large-scale atmospheric circulation patterns favorable for the development of MCS which we haven't investigated. As for the detection of changes in physical variables and environmental parameters, we decided to compare composite fields of daily mean 2 meters-temperature, precipitation, and daily maximum CAPE and DLS but we could consider examining changes in percentiles like Taszarek et al. (2021a) to focus on changes in extreme values, as changes in average conditions can not trivially be linked with changes in extremes. We could also include more convective parameters such as convective inhibition (CIN) or relative humidity. Additionally, the study mainly focused on France and surrounding countries and the results may not be extended to other regions. The potential impact of derechos on society, infrastructure, and people's safety is another area of interest (Ashley and Mote, 2005), that one could investigate in Europe, including the link between derechos and other extreme weather events such as flash floods and heatwaves to gain insights into the potential impact of derechos on society.

Code availability. The code to compute the dynamical indicators of predictability D and persistence Θ is available at https://fr.mathworks.com/matlabcentral/fileexchange/95768-attractor-local-dimension-and-local-persistence-computation.

The Python FLEXible object TRacKeR (PyFLEXTRKR) algorithm developed by Feng et al. (2023a) and is available at https://github.com/FlexTRKR/PyFLEXTRKR.

Other analysis codes and the database of warm-season derechosin France are available upon requests from the authors.

Data availability. ERA5 is the latest climate reanalysis being produced by ECMWF as part of implementing the EU-funded Copernicus Climate Change Service (C3S), providing hourly data on atmospheric, land-surface and sea-state parameters together with estimates of uncertainty from 1979 to present day. ERA5 data for tracking are available on the C3S Climate Data Store on regular latitude-longitude grids at 0.25° x 0.25° resolution have been downloaded from https://cds.climate.copernicus.eu/#!/search?text=ERA5&type=dataset, accessed on 2022-10-30. The ERA5 data for attribution have been downloaded from the preprocessed http://climexp.knmi.nl

The E-OBS dataset from the EU-FP6 project UERRA (http://www.uerra.eu) and the Copernicus Climate Change Service, is available from the ECA&D project (https://www.ecad.eu).

The GPM IMERG Final Precipitation L3 Half Hourly 0.1 degree x 0.1 degree V06 and the NCEP/CPC L3 Half Hourly 4km Global (60S - 60N) Merged IR V1 are available from the Goddard Earth Sciences Data and Information Services Center (GES DISC) respectively at https://doi.org/10.5067/GPM/IMERG/3B-HH/06 and https://doi.org/10.5067/P4HZB9N27EKU.

The European Severe Weather Database (ESWD) from European Severe Storms Laboratory is accessible at https://eswd.eu/.

Weather stations data from Météo-France are available on free request for research https://publitheque.meteo.fr/.

Appendix A: Predictability and Persistence Indices

The attractor of a dynamical system is a geometric object defined in the space hosting all the possible states of the system (phase-space). Each point ζ on the attractor can be characterized by two dynamical indicators: the local dimension D, which indicates the number of degrees of freedom active locally around ζ, and the persistence Θ, a measure of the mean residence time of the system around ζ (Faranda et al., 2017b). To determine D, we exploit recent results from the application of extreme value theory to Poincaré recurrences in dynamical systems. This approach considers long trajectories of a system — in our case successions of daily Z500 latitude–longitude maps — corresponding to a sequence of states on the attractor. For a given point ζ in phase space (e.g., a given Z500 map), we compute the probability that the system returns within a ball of radius ϵ centered on the point ζ. The Freitas et al. (2010) theorem, modified by Lucarini et al. (2012), states that logarithmic returns:

$$g(x(t)) = -\log(\text{dist}(x(t), \zeta)) \tag{A1}$$

yield a probability distribution such that:

$$\Pr(z > s(q)) \simeq \exp\left[-\vartheta(\zeta)\left(\frac{z - \mu(\zeta)}{\sigma(\zeta)}\right)\right] \tag{A2}$$

where $z = g(x(t))$ and s is a high threshold associated to a quantile q of the series $g(x(t))$. Requiring that the orbit falls within a ball of radius ϵ around the point ζ is equivalent to asking that the series $g(x(t))$ is over the threshold s; therefore, the ball radius ϵ is simply $e^{-s(q)}$. The resulting distribution is the exponential member of the Generalized Pareto Distribution family. The parameters μ and σ, namely the location and the scale parameter of the distribution, depend on the point ζ in phase space. $\mu(\zeta)$ corresponds to the threshold $s(q)$ while the local dimension $D(\zeta)$ can be obtained via the relation $\sigma = 1/D(\zeta)$. This is the metric of predictability introduced in Section 2.

When $x(t)$ contains all the variables of the system, the estimation of D based on extreme value theory has a number of advantages over traditional methods (e.g. the box counting algorithm (Liebovitch and Toth, 1989; Sarkar and Chaudhuri, 1994)). First, it does not require to estimate the volume of different sets in scale-space: the selection of $s(q)$ based on the quantile provides a selection of different scales s which depends on the recurrence rate around the point ζ. Moreover, it does not require the a priori selection of the maximum embedding dimension as the observable g is always a univariate time-series.

The persistence of the state ζ is measured via the extremal index $0 < \vartheta(\zeta) < 1$, an adimensional parameter, from which we extract $\Theta(\zeta) = \Delta t/\vartheta(\zeta)$. Here, Δt is the timestep of the dataset being analysed. $\Theta(\zeta)$ is therefore the average residence time of trajectories around ζ, namely the metric of persistence introduced in Section 2, and it has unit of a time (in this study days). If ζ is a fixed point of the attractor, then $\Theta(\zeta) = \infty$. For a trajectory that leaves the neighborhood of ζ at the next time iteration, $\Theta = 1$. To estimate ϑ, we adopt the Süveges estimator (Süveges, 2007). For further details on the the extremal index, see Moloney et al. (2019).

Author contributions.

LF performed the detection and tracking of the derechos and the subsequent analysis. DF performed the attribution analyses. Both authors contributed to discuss the results and write the manuscript.

Competing interests. The authors declare no competing interests

Acknowledgements. The authors thank Bérengère Dubrulle for useful suggestions. The authors also thank Météo-France for providing wind gust data from its weather station network. The authors acknowledge the support of the INSU-CNRS-LEFE-MANU grant (project CROIRE), the grant ANR-20-CE01-0008-01 (SAMPRACE) and support from the European Union's Horizon 2020 research and innovation programme under grant agreement No. 101003469 (XAIDA), and the Marie Sklodowska-Curie grant agreement No. 956396 (EDIPI).

References

Anderson, T. W.: On the distribution of the two-sample Cramer-von Mises criterion, The Annals of Mathematical Statistics, pp. 1148–1159, 1962.

Arguez, A. and Vose, R. S.: The definition of the standard WMO climate normal: The key to deriving alternative climate normals, Bulletin of the American Meteorological Society, 92, 699–704, 2011.

Ashley, W. S. and Mote, T. L.: Derecho Hazards in the United States, Bulletin of the American Meteorological Society, 86, 1577–1592, https://doi.org/10.1175/BAMS-86-11-1577, 2005.

Battaglioli, F., Groenemeijer, P., Púčik, T., Taszarek, M., Ulbrich, U., and Rust, H.: Modelled Multidecadal Trends of Lightning and (Very) Large Hail in Europe and North America (1950–2021), Journal of Applied Meteorology and Climatology, -1, https://doi.org/10.1175/JAMC-D-22-0195.1, 2023.

Bentley, M. L. and Mote, T. L.: A Climatology of Derecho-Producing Mesoscale Convective Systems in the Central and Eastern United States, 1986–95. Part I: Temporal and Spatial Distribution, Bulletin of the American Meteorological Society, 79, 2527–2540, https://doi.org/10.1175/1520-0477(1998)079<2527:ACODPM>2.0.CO;2, 1998.

Bentley, M. L., Mote, T. L., and Byrd, S. F.: A Synoptic Climatology of Derecho Producing Mesoscale Convective Systems in the North-Central Plains, International Journal of Climatology, 20, 1329–1349, https://doi.org/10.1002/1097-0088(200009)20:11<1329::AID-JOC537>3.0.CO;2-F, 2000.

Casanueva, A., Rodríguez-Puebla, C., Frías, M. D., and González-Reviriego, N.: Variability of Extreme Precipitation over Europe and Its Relationships with Teleconnection Patterns, Hydrology and Earth System Sciences, 18, 709–725, https://doi.org/10.5194/hess-18-709-2014, 2014.

Celiński-Mysław, D. and Matuszko, D.: An Analysis of Selected Cases of Derecho in Poland, Atmospheric Research, 149, 263–281, https://doi.org/10.1016/j.atmosres.2014.06.016, 2014.

Celiński-Mysław, D., Palarz, A., and Taszarek, M.: Climatology and Atmospheric Conditions Associated with Cool Season Bow Echo Storms in Poland, Atmospheric Research, 240, 104 944, https://doi.org/10.1016/j.atmosres.2020.104944, 2020.

Christidis, N. and Stott, P. A.: Changes in the Geopotential Height at 500 hPa under the Influence of External Climatic Forcings, Geophysical Research Letters, 42, 10,798–10,806, https://doi.org/10.1002/2015GL066669, 2015.

Coniglio, M. C. and Stensrud, D. J.: Interpreting the Climatology of Derechos, Weather and Forecasting, 19, 595–605, https://doi.org/10.1175/1520-0434(2004)019<0595:ITCOD>2.0.CO;2, 2004.

Coniglio, M. C., Stensrud, D. J., and Richman, M. B.: An Observational Study of Derecho-Producing Convective Systems, Weather and Forecasting, 19, 320–337, https://doi.org/10.1175/1520-0434(2004)019<0320:AOSODC>2.0.CO;2, 2004.

Coppola, E., Nogherotto, R., Ciarlo', J. M., Giorgi, F., van Meijgaard, E., Kadygrov, N., Iles, C., Corre, L., Sandstad, M., and Somot, S.: Assessment of the European climate projections as simulated by the large EURO-CORDEX regional and global climate model ensemble, Journal of Geophysical Research: Atmospheres, 126, e2019JD032 356, iSBN: 2169-897X Publisher: Wiley Online Library, 2021.

Corfidi, S. F., Coniglio, M. C., Cohen, A. E., and Mead, C. M.: A Proposed Revision to the Definition of "Derecho", Bulletin of the American Meteorological Society, 97, 935–949, https://doi.org/10.1175/BAMS-D-14-00254.1, 2016.

Cornes, R. C., van der Schrier, G., van den Besselaar, E. J. M., and Jones, P. D.: An Ensemble Version of the E-OBS Temperature and Precipitation Data Sets, Journal of Geophysical Research: Atmospheres, 123, 9391–9409, https://doi.org/10.1029/2017JD028200, 2018.

Dotzek, N., Groenemeijer, P., Feuerstein, B., and Holzer, A. M.: Overview of ESSL's severe convective storms research using the European Severe Weather Database ESWD, Atmospheric research, 93, 575–586, 2009.

ESSL: The derecho and hailstorms of 18 August 2022, https://www.essl.org/cms/the-derecho-and-hailstorms-of-18-august-2022/, (Accessed on 04-01-2023), 2022.

Evans, J. S. and Doswell, C. A.: Examination of Derecho Environments Using Proximity Soundings, Weather and Forecasting, 16, 329–342, https://doi.org/10.1175/1520-0434(2001)016<0329:EODEUP>2.0.CO;2, 2001.

Faranda, D., Messori, G., Alvarez-Castro, M. C., and Yiou, P.: Dynamical properties and extremes of Northern Hemisphere climate fields over the past 60 years, Nonlinear Processes in Geophysics, 24, 713–725, 2017a.

Faranda, D., Messori, G., and Yiou, P.: Dynamical proxies of North Atlantic predictability and extremes, Scientific reports, 7, 41 278, 2017b.

Faranda, D., Messori, G., and Vannitsem, S.: Attractor dimension of time-averaged climate observables: insights from a low-order ocean-atmosphere model, Tellus A: Dynamic Meteorology and Oceanography, 71, 1–11, 2019.

Faranda, D., Bourdin, S., Ginesta, M., Krouma, M., Messori, G., Noyelle, R., Pons, F., and Yiou, P.: A climate-change attribution retrospective of some impactful weather extremes of 2021, Weather and Climate Dynamics Discussions, pp. 1–37, 2022.

Faranda, D., Messori, G., Jezequel, A., Vrac, M., and Yiou, P.: Atmospheric Circulation Compounds Anthropogenic Warming and Impacts of Climate Extremes in Europe, Proceedings of the National Academy of Sciences, 120, e2214525 120, https://doi.org/10.1073/pnas.2214525120, 2023.

Feng, Z., Leung, L. R., Liu, N., Wang, J., Houze Jr, R. A., Li, J., Hardin, J. C., Chen, D., and Guo, J.: A Global High-Resolution Mesoscale Convective System Database Using Satellite-Derived Cloud Tops, Surface Precipitation, and Tracking, Journal of Geophysical Research: Atmospheres, 126, e2020JD034 202, https://doi.org/10.1029/2020JD034202, 2021.

Feng, Z., Varble, A., Hardin, J., Marquis, J., Hunzinger, A., Zhang, Z., and Thieman, M.: Deep Convection Initiation, Growth, and Environments in the Complex Terrain of Central Argentina during CACTI, Monthly Weather Review, 150, 1135–1155, https://doi.org/10.1175/MWR-D-21-0237.1, 2022.

Feng, Z., Hardin, J., Barnes, H. C., Li, J., Leung, L. R., Varble, A., and Zhang, Z.: PyFLEXTRKR: A Flexible Feature Tracking Python Software for Convective Cloud Analysis, Geoscientific Model Development, 16, 2753–2776, https://doi.org/10.5194/gmd-16-2753-2023, 2023a.

Feng, Z., Leung, L. R., Hardin, J., Terai, C. R., Song, F., and Caldwell, P.: Mesoscale Convective Systems in DYAMOND Global Convection-Permitting Simulations, Geophysical Research Letters, 50, https://doi.org/10.1029/2022GL102603, 2023b.

Freitas, A. C. M., Freitas, J. M., and Todd, M.: Hitting time statistics and extreme value theory, Probability Theory and Related Fields, 147, 675–710, 2010.

Freitas, A. C. M., Freitas, J. M., and Todd, M.: Extreme value laws in dynamical systems for non-smooth observations, Journal of Statistical Physics, 142, 108–126, 2011.

Freitas, A. C. M., Freitas, J. M., and Vaienti, S.: Extreme Value Laws for sequences of intermittent maps, arXiv preprint arXiv:1605.06287, 2016.

Fujita, T. T.: Manual of Downburst Identification for Project NIMROD [National Intensive Meteorological Research on Downburst]., 1978.

Fujita, T. T. and Wakimoto, R. M.: Five Scales of Airflow Associated with a Series of Downbursts on 16 July 1980, Monthly Weather Review, 109, 1438–1456, https://doi.org/10.1175/1520-0493(1981)109<1438:FSOAAW>2.0.CO;2, 1981.

Fumière, Q., Déqué, M., Nuissier, O., Somot, S., Alias, A., Caillaud, C., Laurantin, O., and Seity, Y.: Extreme Rainfall in Mediterranean France during the Fall: Added Value of the CNRM-AROME Convection-Permitting Regional Climate Model, Climate Dynamics, 55, 77–91, https://doi.org/10.1007/s00382-019-04898-8, 2020.

Gatzen, C.: A Derecho in Europe: Berlin, 10 July 2002, Weather and Forecasting, 19, 639–645, https://doi.org/10.1175/1520-0434(2004)019<0639:ADIEBJ>2.0.CO;2, 2004.

Gatzen, C.: Warm-Season Severe Wind Events in Germany, Atmospheric Research, 123, 197–205, https://doi.org/10.1016/j.atmosres.2012.07.017, 2013.

Gatzen, C. P., Fink, A. H., Schultz, D. M., and Pinto, J. G.: An 18-Year Climatology of Derechos in Germany, Natural Hazards and Earth System Sciences, 20, 1335–1351, https://doi.org/10.5194/nhess-20-1335-2020, 2020.

Guastini, C. T. and Bosart, L. F.: Analysis of a Progressive Derecho Climatology and Associated Formation Environments, Monthly Weather Review, 144, 1363–1382, https://doi.org/10.1175/MWR-D-15-0256.1, 2016.

Hamid, K.: Investigation of the Passage of a Derecho in Belgium, Atmospheric Research, 107, 86–105, https://doi.org/10.1016/j.atmosres.2011.12.013, 2012.

Hersbach, H., Bell, B., Berrisford, P., Biavati, G., Horányi, A., Muñoz Sabater, J., Nicolas, J., Peubey, C., Radu, R., Rozum, I., et al.: ERA5 hourly data on single levels from 1959 to present. Copernicus Climate Change Service (C3S) Climate Data Store (CDS), https://doi.org/10.24381/cds.adbb2d47, (Accessed on 09-11-2022), 2018.

Hinrichs, G.: Tornadoes and Derechos, The American Meteorological Journal, 5, 306–317, 341–349, 385–393, 1888.

Hochman, A., Alpert, P., Harpaz, T., Saaroni, H., and Messori, G.: A new dynamical systems perspective on atmospheric predictability: Eastern Mediterranean weather regimes as a case study, Science advances, 5, eaau0936, 2019.

Holley, D., Dorling, S., Steele, C., and Earl, N.: A climatology of convective available potential energy in Great Britain, International Journal of Climatology, 34, 3811–3824, 2014.

Houze, R. A.: 100 Years of Research on Mesoscale Convective Systems, Meteorological Monographs, 59, 17.1–17.54, https://doi.org/10.1175/AMSMONOGRAPHS-D-18-0001.1, 2018.

Huang, B., Thorne, P. W., Banzon, V. F., Boyer, T., Chepurin, G., Lawrimore, J. H., Menne, M. J., Smith, T. M., Vose, R. S., and Zhang, H.-M.: Extended reconstructed sea surface temperature, version 5 (ERSSTv5): upgrades, validations, and intercomparisons, Journal of Climate, 30, 8179–8205, 2017.

Huffman, G., Stocker, E., Bolvin, D., Nelkin, E., and Jackson, T.: GPM IMERG Final Precipitation L3 Half Hourly 0.1 degree x 0.1 degree V06, Greenbelt, MD, Goddard Earth Sciences Data and Information Services Center (GES DISC), https://doi.org/http://doi.org/10.5067/GPM/IMERG/3B-HH/06, 2019.

IPCC: Climate Change 2021: The Physical Science Basis. Contribution of Working Group I to the Sixth Assessment Report of the Intergovernmental Panel on Climate Change, vol. 2, Cambridge University Press, Cambridge, United Kingdom and New York, NY, USA, https://doi.org/10.1017/9781009157896, 2021.

Janowiak, J., Joyce, B., and Xie, P.: NCEP/CPC L3 Half Hourly 4km Global (60S - 60N) Merged IR V1, Edited by Andrey Savtchenko, Greenbelt, MD, Goddard Earth Sciences Data and Information Services Center (GES DISC), https://doi.org/http://doi.org/10.5067/P4HZB9N27EKU, 2017.

Johns, R. H. and Hirt, W. D.: The Derecho of July 19–20, 1983. A Case Study, National Weather Digest, 10, 17–32, 1985.

Johns, R. H. and Hirt, W. D.: Derechos: Widespread Convectively Induced Windstorms, Weather and Forecasting, 2, 32–49, https://doi.org/10.1175/1520-0434(1987)002<0032:DWCIW>2.0.CO;2, 1987.

Kunkel, K. E., Karl, T. R., Brooks, H., Kossin, J., Lawrimore, J. H., Arndt, D., Bosart, L., Changnon, D., Cutter, S. L., Doesken, N., Emanuel, K., Groisman, P. Y., Katz, R. W., Knutson, T., O'Brien, J., Paciorek, C. J., Peterson, T. C., Redmond, K., Robinson, D., Trapp, J., Vose, R., Weaver, S., Wehner, M., Wolter, K., and Wuebbles, D.: Monitoring and Understanding Trends in Extreme Storms: State of Knowledge, Bulletin of the American Meteorological Society, 94, 499–514, https://doi.org/10.1175/BAMS-D-11-00262.1, 2013.

Lewis, M. W. and Gray, S. L.: Categorisation of synoptic environments associated with mesoscale convective systems over the UK, Atmospheric Research, 97, 194–213, 2010.

Liebovitch, L. S. and Toth, T.: A fast algorithm to determine fractal dimensions by box counting, physics Letters A, 141, 386–390, 1989.

López, J. M.: A Mediterranean Derecho: Catalonia (Spain), 17th August 2003, Atmospheric Research, 83, 272–283, https://doi.org/10.1016/j.atmosres.2005.08.008, 2007.

Lucarini, V., Faranda, D., and Wouters, J.: Universal behaviour of extreme value statistics for selected observables of dynamical systems, Journal of statistical physics, 147, 63–73, 2012.

Lucarini, V., Faranda, D., Freitas, A. C. M., Freitas, J. M., Holland, M., Kuna, T., Nicol, M., Todd, M., and Vaienti, S.: Extremes and recurrence in dynamical systems, John Wiley & Sons, 2016.

Markowski, P. and Richardson, Y.: Mesoscale Meteorology in Midlatitudes, Wiley, 1 edn., https://doi.org/10.1002/9780470682104, 2010.

Mathias, L., Ludwig, P., and Pinto, J. G.: Synoptic-Scale Conditions and Convection-Resolving Hindcast Experiments of a Cold-Season Derecho on 3 January 2014 in Western Europe, Natural Hazards and Earth System Sciences, 19, 1023–1040, https://doi.org/10.5194/nhess-19-1023-2019, 2019.

Messori, G., Caballero, R., and Faranda, D.: A dynamical systems approach to studying midlatitude weather extremes, Geophysical Research Letters, 44, 3346–3354, 2017.

Moloney, N. R., Faranda, D., and Sato, Y.: An overview of the extremal index, Chaos: An Interdisciplinary Journal of Nonlinear Science, 29, 022 101, 2019.

Morris, R.: The Spanish plume-testing the forecasters nerve, Meteorological Magazine, 115, 349–357, 1986.

Natalia Pilguj, Mateusz Taszarek, John T. Allen, and Kimberly A. Hoogewind: Are Trends in Convective Parameters over the United States and Europe Consistent between Reanalyses and Observations?, Journal of Climate, pp. 1–52, https://doi.org/10.1175/jcli-d-21-0135.1, 2022.

Nobre, G. G., Jongman, B., Aerts, J., and Ward, P. J.: The role of climate variability in extreme floods in Europe, Environmental Research Letters, 12, 084 012, 2017.

Púčik, T., Francová, M., Rýva, D., Kolář, M., and Ronge, L.: Forecasting Challenges during the Severe Weather Outbreak in Central Europe on 25 June 2008, Atmospheric Research, 100, 680–704, https://doi.org/10.1016/j.atmosres.2010.11.014, 2011.

Púčik, T., Groenemeijer, P., Rädler, A. T., Tijssen, L., Nikulin, G., Prein, A. F., van Meijgaard, E., Fealy, R., Jacob, D., and Teichmann, C.: Future Changes in European Severe Convection Environments in a Regional Climate Model Ensemble, Journal of Climate, 30, 6771–6794, https://doi.org/10.1175/JCLI-D-16-0777.1, 2017.

Punkka, A.-J., Teittinen, J., and Johns, R. H.: Synoptic and Mesoscale Analysis of a High-Latitude Derecho–Severe Thunderstorm Outbreak in Finland on 5 July 2002, Weather and Forecasting, 21, 752–763, https://doi.org/10.1175/WAF953.1, 2006.

Ribes, A., Thao, S., Vautard, R., Dubuisson, B., Somot, S., Colin, J., Planton, S., and Soubeyroux, J.-M.: Observed Increase in Extreme Daily Rainfall in the French Mediterranean, Climate Dynamics, 52, 1095–1114, https://doi.org/10.1007/s00382-018-4179-2, 2019.

Sarkar, N. and Chaudhuri, B. B.: An efficient differential box-counting approach to compute fractal dimension of image, IEEE Transactions on systems, man, and cybernetics, 24, 115–120, 1994.

Schulz, W., Diendorfer, G., Pedeboy, S., and Poelman, D. R.: The European Lightning Location System EUCLID – Part 1: Performance Analysis and Validation, Natural Hazards and Earth System Sciences, 16, 595–605, https://doi.org/10.5194/nhess-16-595-2016, 2016.

Schumacher, R. S. and Rasmussen, K. L.: The Formation, Character and Changing Nature of Mesoscale Convective Systems, Nature Reviews Earth & Environment, 1, 300–314, https://doi.org/10.1038/s43017-020-0057-7, 2020.

Squitieri, B. J., Wade, A. R., and Jirak, I. L.: A Historical Overview on the Science of Derechos. Part 1: Identification, Climatology, and Societal Impacts, Bulletin of the American Meteorological Society, https://doi.org/10.1175/BAMS-D-22-0217.1, 2023.

Stein, C. and Wald, A.: Sequential confidence intervals for the mean of a normal distribution with known variance, The Annals of Mathematical Statistics, pp. 427–433, 1947.

Süveges, M.: Likelihood estimation of the extremal index, Extremes, 10, 41–55, 2007.

Taszarek, M., Allen, J., Púčik, T., Groenemeijer, P., Czernecki, B., Kolendowicz, L., Lagouvardos, K., Kotroni, V., and Schulz, W.: A Climatology of Thunderstorms across Europe from a Synthesis of Multiple Data Sources, Journal of Climate, 32, 1813–1837, https://doi.org/10.1175/JCLI-D-18-0372.1, 2019.

Taszarek, M., Allen, J. T., Púčik, T., Hoogewind, K. A., and Brooks, H. E.: Severe Convective Storms across Europe and the United States. Part II: ERA5 Environments Associated with Lightning, Large Hail, Severe Wind, and Tornadoes, Journal of Climate, 33, 10 263–10 286, https://doi.org/10.1175/JCLI-D-20-0346.1, 2020.

Taszarek, M., Allen, J. T., Brooks, H. E., Pilguj, N., and Czernecki, B.: Differing Trends in United States and European Severe Thunderstorm Environments in a Warming Climate, Bulletin of the American Meteorological Society, 102, E296–E322, https://doi.org/10.1175/BAMS-D-20-0004.1, 2021a.

Taszarek, M., Allen, J. T., Marchio, M., and Brooks, H. E.: Global Climatology and Trends in Convective Environments from ERA5 and Rawinsonde Data, npj Climate and Atmospheric Science, 4, 1–11, https://doi.org/10.1038/s41612-021-00190-x, 2021b.

Trenberth, K. E. and Shea, D. J.: Atlantic hurricanes and natural variability in 2005, Geophysical research letters, 33, 2006.

van Delden, A.: The Synoptic Setting of Thunderstorms in Western Europe, Atmospheric Research, 56, 89–110, https://doi.org/10.1016/S0169-8095(00)00092-2, 2001.

Wei, W., Yan, Z., and Li, Z.: Influence of Pacific Decadal Oscillation on Global Precipitation Extremes, Environmental Research Letters, 16, 044 031, https://doi.org/10.1088/1748-9326/abed7c, 2021.

Wikipedia: 2022 European derecho, https://en.wikipedia.org/wiki/2022_European_derecho, (Accessed on 04-01-2023), 2022.

Yang, Q., Houze Jr, R. A., Leung, L. R., and Feng, Z.: Environments of Long-Lived Mesoscale Convective Systems Over the Central United States in Convection Permitting Climate Simulations, Journal of Geophysical Research: Atmospheres, 122, 13,288–13,307, https://doi.org/10.1002/2017JD027033, 2017.

Zampieri, M., Toreti, A., Schindler, A., Scoccimarro, E., and Gualdi, S.: Atlantic multi-decadal oscillation influence on weather regimes over Europe and the Mediterranean in spring and summer, Global and Planetary Change, 151, 92–100, 2017.

Zhuang, J., dussin, r., Huard, D., Bourgault, P., Banihirwe, A., Raynaud, S., Malevich, B., Schupfner, M., Filipe, Levang, S., Gauthier, C., Jüling, A., Almansi, M., RichardScottOZ, RondeauG, Rasp, S., Smith, T. J., Stachelek, J., Plough, M., Pierre, Bell, R., Caneill, R., and Li, X.: Pangeo-Data/xESMF: V0.8.2, Zenodo, https://doi.org/10.5281/zenodo.8356796, 2023.

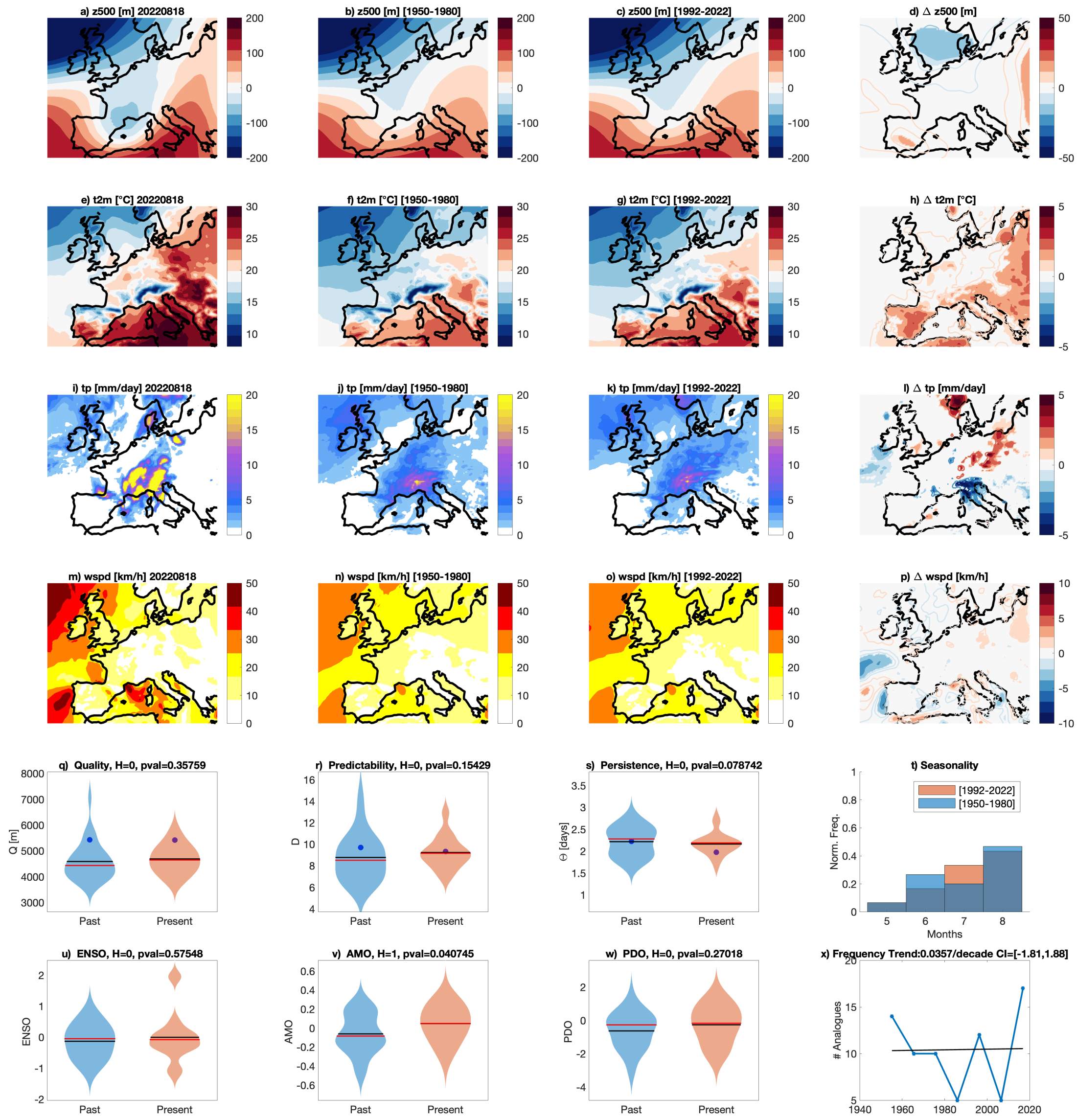

Figure 4. Attribution for the 18 August 2022 derecho storm. Daily mean zero-centered geopotential height anomaly (z500) (a), 2-meter temperatures t2m (e), total precipitation tp (i), wind-speed wspd (m) on the day of the event. Average of the 29 sea-level pressure analogues found for the counterfactual [1950-1980] (b) and factual [1992-2022] (c) periods and corresponding 2-meter temperatures (f,g), daily precipitation rate (j,k) and wind speed (n,o). ΔZ500 (d), Δt2m (h), Δtp (i) and Δwspd (p) between factual and counterfactual periods: colored-filled areas show significant anomalies with respect to the bootstrap procedure. Violin plots for counterfactual (blue) and factual (orange) periods for the analogues Quality Q (q) the Predictability index D (r), the Persistence index Θ (s) and the distribution of analogues in each month (t). Violin plots for counterfactual (blue) and factual (orange) periods for ENSO (u), AMO (v) and PDO (w). The number of analogues per decade (blue) and its linear trend (black) in (x). Values for the peak day of the extreme event are marked by a dot. Titles in (q–v) report the results of the Cramér-von Mises test H and the pvalue pval. Title in panel (w) includes the value of the linear trend slope and its confidence interval CI in square brackets.

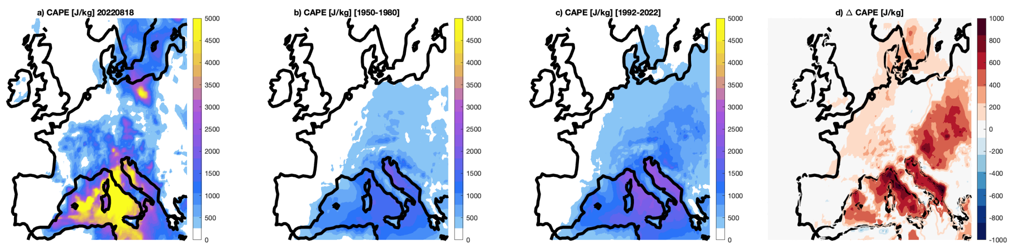

Figure 5. As in Figure 4 but for daily maximum CAPE.

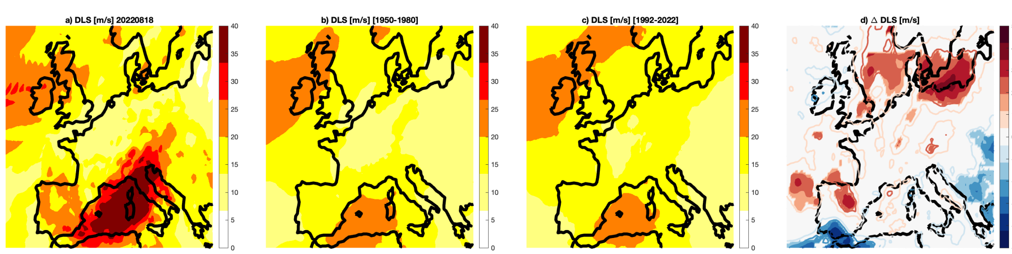

Figure 6. As in Figure 4 but for daily maximum DLS.